Published in final edited form as:
Cell Rep. 2014 July 24; 8(2): 487–500. doi:10.1016/j.celrep.2014.06.031.

Sox4 Links Tumor Suppression to Accelerated Aging in Mice by Modulating Stem Cell Activation

Miguel Foronda[1], **Paula Martínez**[1], **Stefan Schoeftner**[1,4], **Gonzalo Gómez-López**[2], **Ralph Schneider**[1], **Juana M. Flores**[3], **David G. Pisano**[2], and **Maria A. Blasco**[1,*]

[1]Telomeres and Telomerase Group, Molecular Oncology Program

[2]Bioinformatics Unit, Biotechnology Program Spanish National Cancer Research Centre (CNIO), Madrid 28029, Spain

[3]Department of Animal Surgery and Pathology, Complutense University of Madrid, Madrid 28040, Spain

Summary

Sox4 expression is restricted in mammals to embryonic structures and some adult tissues, such as lymphoid organs, pancreas, intestine, and skin. During embryogenesis, Sox4 regulates mesenchymal and neural progenitor survival, as well as lymphocyte and myeloid differentiation, and contributes to pancreas, bone, and heart development. Aberrant Sox4 expression is linked to malignant transformation and metastasis in several types of cancer. To understand the role of Sox4 in the adult organism, we first generated mice with reduced whole-body Sox4 expression. These mice display accelerated aging and reduced cancer incidence. To specifically address a role for Sox4 in adult stem cells, we conditionally deleted *Sox4* (*Sox4*^{cKO}) in stratified epithelia. *Sox4*^{cKO} mice show increased skin stem cell quiescence and resistance to chemical carcinogenesis concomitantly with downregulation of cell cycle, DNA repair, and activated hair follicle stem cell pathways. Altogether, these findings highlight the importance of Sox4 in regulating adult tissue homeostasis and cancer.

Introduction

Adult organs are maintained through a balance of proliferation, differentiation, and self-renewal of stem cells that take place during normal tissue homeostasis or to repair tissue damage (Sharpless and DePinho, 2007). Alterations in this equilibrium can result in

*Correspondence: mblasco@cnio.es.
[4]Present address: Laboratorio Nazionale Consorzio Interuniversitario Biotecnologie (LNCIB), Telomeres in Cancer and Aging Unit, Padriciano 99, Trieste 34149, Italy

Accession Numbers
The microarray data sets reported in this paper have been deposited in the GEO database under accession number GSE58155.

Author Contributions
M.A.B. secured funding, interpreted results, designed experiments, and wrote the manuscript. M.F. designed and performed most of the experiments, interpreted results, and wrote the manuscript. P.M. performed experiments and wrote the manuscript. R.P.S. and S.S. contributed with intellectual input. G.G.-L. and D.G.-P. performed the bioinformatics analysis. J.-M.F. performed the histopathological analysis.

decreased organ function and are linked to degenerative processes such as cancer and aging (Garinis et al., 2008; Hoeijmakers, 2009; López-Otín et al., 2013).

The skin is the largest of all the mammalian organs and its principal function is to provide protection from external aggressions and dehydration (Fuchs, 2007). It is composed of a supportive connective tissue (dermis) and a stratified epithelium (epidermis). The epithelium comprises the interfollicular epidermis (IFE) and its appendages, namely, the sebaceous glands (SGs) and the hair follicles (HFs) (Blanpain and Fuchs, 2009; Watt, 2001). The epidermis is very dynamic and is maintained through bouts of activation of its stem cells, located in the HFs (HF stem cells [HFSCs]) in the bulge and hair germ (HG) regions, which are identified by expression of CD34, cytokeratin 15, and Lgr5 markers (Greco et al., 2009; Hsu et al., 2011; Solanas and Benitah, 2013). HFSC activation occurs throughout the entire life of the organism during the hair cycle, which alternates among resting (telogen), proliferation and differentiation (anagen), and destructive (catagen) phases (Alonso and Fuchs, 2006; Müller-Röver et al., 2001). The alternation among these states is orchestrated by the dermal papilla, which provides the signals required for HFSC activation to the lower-bulge and HG stem cells through the TGFβ, Notch, and Wnt/*Ctnnb1* pathways (Greco et al., 2009; Lien et al., 2014; Oshimori and Fuchs, 2012; Rendl et al., 2008; Solanas and Benitah, 2013). Upper-bulge stem cells (whose markers include *Gli1*, *Lrig1*, and *Lgr6*, among others) also rely on Shh signals to contribute to IFE replenishment during wound repair, but not to HF cycling (Jensen et al., 2009; Solanas and Benitah, 2013). The molecular signature of resting and activated HFSCs has been extensively studied by transcriptional profiling. The results showed that whereas dormant HFSCs are enriched in factors that promote quiescence and/or self-renewal, including *Lhx2*, *Lgr5*, *Lgr6*, *Lrig1*, and CD34, among others (Braun et al., 2003; Jaks et al., 2008; Jensen et al., 2009, 2010; Nowak et al., 2008; Rhee et al., 2006; Snippert et al., 2010), activation of HFSCs occurs in a stepwise manner with increased expression of genes controlled by the canonical Wnt/*Ctnnb1* pathway, most of which are involved in cell-cycle progression, differentiation, extracellular matrix/adhesion, and transcription (Greco et al., 2009; Lien et al., 2014). Among them, *Sox4* (*Sry*-related High Mobility Group [HMG] box-containing transcription factor 4) was found to be upregulated 5-fold by microarray-based transcriptional profiling (Greco et al., 2009; Kobielak et al., 2007; Lien et al., 2014; Lowry et al., 2005).

Sox4 belongs to the SoxC class of transcription factors, encompassing Sox4, Sox11, and Sox12 (Harley and Lefebvre, 2010). Sox4 is expressed mainly during embryonic development in the neural crest, mesenchyme, developing pancreas, thymus, spleen, and HFs (Dy et al., 2008; Hoser et al., 2008; Lioubinski et al., 2003). In adults, Sox4 expression is found in a limited set of tissues, including the female reproductive system, hematopoietic system, pancreatic islets, intestinal crypts, and activated HFSCs and HG cells (Deneault et al., 2009; Greco et al., 2009; Hunt and Clarke, 1999; Lien et al., 2014; Lowry et al., 2005; Schilham et al., 1997; Van der Flier et al., 2007; Wilson et al., 2005). The main functions attributed to Sox4 are the regulation of survival and proliferation of neural and mesenchymal progenitors (Bhattaram et al., 2010), cardiac outflow formation (Schilham et al., 1996), pancreatic islet and osteoblast development (Nissen-Meyer et al., 2007; Wilson et al., 2005), B and T cell maturation (Kuwahara et al., 2012; Schilham et al., 1997), and myeloid differentiation (Aue et al., 2011; Sandoval et al., 2012). The constrictions in expression of

Sox4 by adult cells suggest that a tight regulation is required to maintain an adequate tissue homeostasis. Indeed, aberrant Sox4 expression in adult tissues is linked to cancer onset and progression in mice and humans (Jafarnejad et al., 2013; Vervoort et al., 2013).

The first proof that Sox4 could act as an oncogene was the finding that the *Sox4* locus is one of the common integration sites in genome-wide tagging protocols based on retroviral-mediated activation of proto-oncogenes (Du et al., 2005; Li et al., 2007; Shin et al., 2004). Since then, Sox4 overexpression has been found in virtually all major cancer types, including lung, bladder, prostate, hepatic, gastric, neural, and hematopoietic cancers (Vervoort et al., 2013). Overexpression of Sox4 is sufficient to induce transformation in the hematopoietic compartment by blocking myeloid differentiation (Aue et al., 2011; Boyd et al., 2006; Omidvar et al., 2013; Sandoval et al., 2012; Zhang et al., 2013). Furthermore, Sox4 inhibits apoptosis and increases cell proliferation (Hur et al., 2010). Interestingly, abrogation of Sox4 in medulloblastoma cell lines increases their sensitivity to ionizing radiation (IR), indicating that this protein confers DNA damage resistance to this type of cancer cells (Chetty et al., 2012). Finally, Sox4 is crucial in different steps of metastatic colonization, being regulated through the Wnt pathway, transforming growth factor β (TGF-β) cues and endogenous miRNAs to promote epithelial-to-mesenchymal transition (EMT) through Ezh2-mediated epigenetic reprogramming and regulation of cancer cell proliferation (Parvani and Schiemann, 2013; Tavazoie et al., 2008; Tiwari et al., 2013; Vervoort et al., 2013).

Several mouse models for studying Sox4 have been generated. *Sox4-null* (*Sox4*$^{-/-}$) mice die in utero at embryonic day 14.5 (E14.5) bearing cardiac malformations, incomplete pancreatic islet development, and defects in lymphoid maturation (Schilham et al., 1996). *Sox4*$^{+/-}$ mice show decreased bone mineralization due to impaired osteoblast development (Nissen-Meyer et al., 2007). *Sox4* deletion in hematopoietic cells results in impaired B and T cell maturation and its overexpression blocks myeloid differentiation (Kuwahara et al., 2012; Sun et al., 2013; Zhang et al., 2013). A recent report also showed that *Sox4* deletion in renal progenitors results in premature kidney dysfunction (Huang et al., 2013).

Sox4 is the only SoxC class member that is expressed in skin. In particular, Sox4 has been detected in the upper and lower bulge in HFs during morphogenesis at E18.5 (Dy et al., 2008), during the telogen-to-anagen transition in activated HFSCs from the bulge and HG (Greco et al., 2009; Lien et al., 2014; Lowry et al., 2005), and in E6/E7 oncogene-mediated or *Bmpr1*^{cKO}-driven activated HFSCs (da Silva-Diz et al., 2013; Kobielak et al., 2007). Specifically, Sox4 responds to canonical Wnt signals in activated HFSCs in a *Ctnnb1*-sensitive manner during hair regeneration after plucking (Lien et al., 2014). Nevertheless, the functions of Sox4 in most adult tissues, and particularly in skin homeostasis and cancer, remain largely unknown.

Here, we sought to address the roles of Sox4 in adult tissue homeostasis and cancer. We generated a mouse model with downregulated expression of *Sox4* in most tissues (*Sox4*$^{lox/lox}$ mice). These mice are viable and fertile, but are smaller in size than their wild-type (WT) littermates. Hypomorphic *Sox4*$^{lox/lox}$ mice develop a panel of premature age-associated pathologies and a significantly reduced longevity. In addition, these mice are

cancer resistant. Specific deletion of Sox4 in skin (*Sox4*^{cKO} mice) results in normal skin stratification. However, Sox4 deficiency in skin hampers normal HFSC activation upon forced proliferative cues. When subjected to a chemically induced skin carcinogenesis protocol, *Sox4*^{cKO} mice show a strong resistance to tumor development. Finally, we explain these phenotypes by identifying a *Sox4*-associated transcriptional regulation of gene sets associated with cell division, DNA repair, and HFSC activation. Altogether, our results shed light on some crucial functions of this protein in cancer and aging and provide new tools for elucidating Sox4 function in adult tissues.

Results

Generation of Knockin *Sox4* Mice

The fact that complete *Sox4* abrogation (*Sox4*$^{-/-}$ mice) results in embryonic lethality (Schilham et al., 1996) has hampered efforts to understand the role of Sox4 in the adult organism. To circumvent this, we decided to generate a *Sox4* knockin (KI) mouse model (*Sox4*$^{lox/lox}$ mice) that would allow us to track *Sox4*-expressing cells in vivo and conditionally delete *Sox4* in adult tissues. To that end, we generated a KI construct targeted to the *Sox4* locus, including the whole *Sox4* 5’ UTR and 3’ UTR and the full-length *Sox4* unique exon adjacent to an IRES-FP-Luciferase (GFP-Luc) reporter coding sequence. We flanked the KI allele with LoxP sites in order to allow the excision of the whole cassette with tissue-specific *Cre* recombinase. When intact, the KI cassette is regulated by the endogenous *Sox4* promoter, and its transcription is expected to give rise to the full-length Sox4 protein and the GFP-Luc reporter simultaneously (Figures 1A and 1B).

Sox4 $^{lox/lox}$ Mice Show Signs of Premature Aging and Are Cancer Resistant

The *Sox4*$^{lox/lox}$ mice were viable and fertile and did not show signs of embryonic lethality at E13.5 or E18.5; however, they displayed sub-Mendelian ratios at weaning (Figure S1A), suggesting a selection in the litters. We attributed this to the delayed weight and size gain in the earliest postnatal stages (Figures S1B and S1C). The reduced body size and weight of *Sox4*$^{lox/lox}$ mice was maintained through their entire lifespan (Figures 1C and 1D). Dual-energy X-ray absorptiometry (DEXA) indicated that the reduced weight was due to a decrease in both lean and fat mass (Figures S1D–S1F). In addition, *Sox4*$^{lox/lox}$ mice had a significantly reduced longevity when compared with *Sox4*$^{+/+}$ or *Sox4*$^{+/lox}$ mice (Figures 1E and S1G). This decreased survival paralleled the early onset of various age-associated pathologies. In particular, *Sox4*$^{lox/lox}$ mice presented decreased bone mineral density (Figure 1F) and a higher incidence of intestinal failure, chronic hepatic failure, skin hyperpigmentation, and dilated cardiomyopathy (Figures 1C and 1G; Table S1). We also found a significantly increased incidence of congenital diaphragmatic hernia and pyometra (Figure 1G; Table S1). Furthermore, the humane endpoint (HEP) was reached significantly earlier in *Sox4*$^{lox/lox}$ compared with control mice (Figures 1E and S1G; Table S1). This reduced longevity coincided with a notable reduction in the mean telomere length of peripheral blood cells, a bona fide indicator of biological aging (Canela et al., 2007; de Jesus and Blasco, 2012; López-Otín et al., 2013; Vera et al., 2012; Figure 1H). Interestingly, these mice displayed a reduced spontaneous cancer incidence when compared with *Sox4*$^{+/+}$ mice (Figure 1I). Together, these findings indicate that *Sox4*$^{lox/lox}$ mice show signs of premature

loss of tissue homeostasis and subsequently an accelerated onset of age-associated pathologies concomitantly with cancer resistance.

Sox4 $^{lox/lox}$ Mice Are Hypomorphic

The above results showed that the *Sox4* KI allele exhibits hypomorphic behavior. In order to confirm this, we performed indirect immunohistochemistry (IHC) for GFP in tail skin sections, given that *Sox4* mRNA has been detected in skin (Dy et al., 2008; Greco et al., 2009; Lowry et al., 2005). We failed to detect any positive GFP signal (Figure S2A), indicating either very low expression levels of the KI cassette or decreased *Sox4* expression in adult mouse skin. To quantify *Sox4* mRNA expression levels in *Sox4* $^{lox/lox}$ mice, we performed *Sox4* real-time quantitative RT-PCR (qPCR) in a panel of tissues from both *Sox4* $^{lox/lox}$ and *Sox4* $^{+/+}$ mice. *Sox4* $^{lox/lox}$ mice showed an ~10-fold reduction in *Sox4* mRNA levels in all analyzed tissues when compared with WT littermates (Figure 1J). Of note, we did not detect a high variability in *Sox4* expression levels among the *Sox4* $^{lox/lox}$ mice tested, indicating that the *Sox4* hypomorphic allele is expressed similarly in surviving adult mice (Figure S2B). Notably, we did not detect any significant deregulation of the other *SoxC* class members (*Sox11* and *Sox12*) in the analyzed tissues (Figure S2C). Altogether, these findings demonstrate that the *Sox4* $^{lox/lox}$ mouse model described herein behaves as a functional hypomorph for *Sox4* mRNA expression levels and thus constitutes a viable adult mouse model with whole-body reduced *Sox4* expression.

Generation of a *Sox4* Conditional KO Mouse Model in Stratified Epithelia

The above results indicate that adult mice with reduced *Sox4* levels show a faster loss of normal tissue homeostasis. As the latter relies on a controlled balance between tissue replenishment and degeneration, we hypothesized that organ failure could be due to defects in the activity of adult stem cells. Up to now, *Sox4* has been the only *SoxC* class member shown to be expressed in developing and adult skin, mostly in activated HFSCs and HG during the telogen-to-anagen transition (Dy et al., 2008; Greco et al., 2009; Lien et al., 2014; Lowry et al., 2005). Moreover, *Sox4* $^{lox/lox}$ mice showed an increased incidence of skin hyperpigmentation at the HEP (Figure 1C; Table S1) and a delayed onset of the placode-to-HF transition during hair morphogenesis (Figure S2D), with the latter suggesting delayed activation of HFSCs (Nowak et al., 2008). In order to test this, we abrogated *Sox4* in skin to model adult stem cell function. We crossed *Sox4* $^{lox/lox}$ mice with *K5-Cre* transgenic mice (Ramirez et al., 2004), giving rise to *Sox4* $^{+/+}$; *K5-Cre* $^{Tg/+}$ (*Sox4* ^{WT}) and *Sox4* $^{lox/lox}$; *K5-Cre* $^{Tg/+}$ (*Sox4* ^{cKO}) mice. As expected, the *Sox4* ^{cKO} mice were viable and lacked *Sox4* mRNA expression in tail skin epidermis when compared with *Sox4* ^{WT}, and showed no differences in *Sox11* and *Sox12* (Figures 2A, 2B, and S3A). Of note, we did not find any significant change in the lifespan of *Sox4* $^{+/+}$; K5Cre $^{Tg/+}$ when compared with *Sox4* $^{+/+}$; K5Cre $^{+/+}$ mice, *Sox4* $^{+/lox}$; K5Cre $^{Tg/+}$ (*Sox4* ^{cHET}) compared with *Sox4* $^{+/lox}$; K5Cre $^{+/+}$ mice, or *Sox4* $^{lox/lox}$; K5Cre $^{Tg/+}$ versus *Sox4* $^{lox/lox}$; K5Cre $^{+/+}$ mice (Figure S3B). Therefore, unless specifically mentioned otherwise, hereafter we refer to *Sox4* $^{+/+}$; K5Cre $^{Tg/+}$ and *Sox4* $^{+/+}$; K5Cre $^{+/+}$ mice collectively as *Sox4* ^{WT} mice.

Europe PMC Funders Author Manuscripts

Sox4 Is Dispensable for Normal Skin Stratification

In order to assess the role of *Sox4* in skin, we studied several differentiation markers in *Sox4*^{cKO} and *Sox4*^{WT} mice. We did not find differences in the assembly or disposition of cytokeratin 10 (CK10, committed basal keratinocytes), CK14 (epidermal keratinocytes), or loricrin (terminally differentiated, cornified layer of keratinocytes) (Fuchs, 1994; Figure 2C). In addition, *Sox4*^{cKO} mice displayed a normal hair coat upon gross examination (Figure 2A), indicating that *Sox4* is largely dispensable for normal skin stratification. Finally, since *Sox4*^{cKO} mice were hypomorphic for Sox4 expression in the rest of the tissues, they also displayed a reduced size, decreased weight, and shorter lifespan, thus recapitulating the phenotypes observed in *Sox4*$^{lox/lox}$ mice (Figures S3B–S3D).

Decreased Replicative History in Sox4-Depleted Bulge Cells

Sox4 is expressed in the skin in adult stem cell compartments such as the bulge and HG upon physiological or forced HFSC activation, including hair morphogenesis, normal hair cycling, plucking-induced anagen, *Bmpr1*^{cKO}-mediated HFSC activation, and oncogenic E6/E7-driven bulge stem cell mobilization (da Silva-Diz et al., 2013; Dy et al., 2008; Greco et al., 2009; Kobielak et al., 2007; Lien et al., 2014; Lowry et al., 2005). Moreover, Sox4 has been strongly linked to regulation of stem cell activity by controlling crucial steps such as differentiation and induction proliferation (Lefebvre et al., 2007). Therefore, we aimed to address whether Sox4 could also modulate HFSC activity. We reasoned that the effects of such regulation should become evident in the long term, and thus we measured telomere length as a molecular indicator of the replicative history of the cells (López-Otín et al., 2013). For this purpose, we performed quantitative fluorescence in situ hybridization (QFISH), which allows the determination of telomere length at a single-cell resolution (Flores et al., 2008), in tail skin sections from 6-month-old mice. We observed longer telomeres in the hair bulge of *Sox4*^{cKO} mice as compared with WT controls, as reflected by an increased mean telomere length and accumulation of long telomeres (Figures 2D and 2E). These results are suggestive of a decreased replicative history in *Sox4*-depleted HFSCs (Flores et al., 2008).

Sox4 Is Upregulated during Plucking and Is Required for Normal Hair Regeneration

It is possible to force unscheduled entry into the hair cycle by physically removing a portion of the hair coat. Following plucking, resting HFSCs and HG cells exit quiescence, become activated, and proliferate while differentiating into all the hair lineages (Keyes et al., 2013; Lien et al., 2014; Müller-Röver et al., 2001). This activation of HFSCs is accompanied by changes in their gene-expression signature such as upregulation of canonical Wnt/*Ctnnb1* signaling-related genes, including *Sox4* (Greco et al., 2009; Lien et al., 2014; Lowry et al., 2005). To explore *Sox4* expression dynamics during the plucking-induced telogen-to-anagen transition, we depilated a group of *Sox4*^{WT} mice and determined the mRNA expression levels for several markers of HFSC activity. We found upregulation of *GATA3*, *Tcf3/4*, *mTERT*, *Sox9*, and *c-Myc* mRNA in a stepwise manner, confirming sequential activation of HFSCs after plucking (Greco et al., 2009; Figure 3A). *Sox4* was similarly induced during hair regeneration (Figure 3B). None of the other *SoxC* class members showed significant changes after plucking, indicating a functional specificity of Sox4 in the context of HFSC

activation (Figure 3B). These results confirm that *Sox4* is among the genes that are induced during activation of HFSCs. To test whether *Sox4* is required for hair regeneration, we plucked *Sox4*^{WT} and *Sox4*^{cKO} mice. We observed complete fur regeneration in *Sox4*^{WT} mice 12–15 days after plucking, whereas *Sox4*^{cKO} mice displayed a delayed hair growth (Figure 3C).

The delay in hair regeneration together with the reduced replicative history of HFSC in *Sox4*^{cKO} mouse skin suggests that Sox4 may be an important modulator of HFSC activation and thus could serve relevant functions during skin regeneration.

Delayed HFSC Activation in the Absence of *Sox4*

We wanted to test the ability of HFSCs to regenerate the skin in the absence of Sox4 (Keyes et al., 2013; Müller-Röver et al., 2001). To this end, we performed skin histology and IHC analysis 12 days after plucking. First, we noted a significant reduction in HF length, epidermal thickness, and dermis size in *Sox4*^{cKO} compared with *Sox4*^{WT}, suggestive of diminished hair cycle induction in the absence of Sox4 (Figures 4A and 4B; Flores et al., 2005; Keyes et al., 2013; Müller-Röver et al., 2001). Simultaneously, there was an overall decrease in the number of proliferating cells as evidenced by Ki67 staining in several skin regions, including the hair bulb and the hair progeny compartments, further supporting limited induction of hair cycling (Figures 4C and 4D). This was accompanied by an increase in the percentage of γH2AX-positive cells (Figures 4E and 4F) and p53-positive cells, especially in activated HFSC compartments such as the junctional zone (JZ) and the bulge (Figures 4G and 4H). To confirm that Sox4 was required for HFSC differentiation, we extracted total keratinocytes from newborn and adult mice and cultured them under clonogenic conditions in which only stem cells can proliferate and differentiate, generating large colonies arising from single cells (Blanco et al., 2011; Jensen et al., 2010). After 2 weeks in culture, we observed a significant reduction in the number of large, differentiated colonies in keratinocytes bearing reduced expression of *Sox4* in a dose-and age-dependent manner (Figures 4I and S4A).

In mice, hair regeneration relies on the activity of HFSCs located in the hair bulge and HG (Fuchs, 2009; Greco et al., 2009). Other HFSC populations can also contribute to tissue replenishment in regions other than the hair. Among them, JZ/Lrig1-positive cells can provide input to the IFE under wounding stimuli (Jensen et al., 2009). In order to specifically test whether Sox4 also could be required for proper IFE regeneration upon wounding, we performed wound-healing assays. In accordance with delayed hair regeneration, *Sox4*^{cKO} mice also displayed a significant slowdown in replenishing the epidermis after wounding (Figure 4J). This supports a general delayed response of *Sox4*-deficient skin to proliferative stimuli in several HFSC/multipotent skin compartments and thus accounts for the reduced regenerative capacity of several skin compartments.

Finally, we confirmed that both *Sox4*^{WT} and *Sox4*^{cKO} mice had similar numbers of HFSCs, as indicated by a similar total number of colonies (including small, undifferentiated ones) in the clonogenic assays and by equal numbers of label-retaining cells (Braun et al., 2003; Figures S4A and S4B). Together with the delayed hair morphogenesis, these results indicate

that Sox4 plays a central role in modulating HFSC differentiation, but not during HFSC specification and/or self-renewal.

Sox4 Is Required for the Coordinated Initiation of HFSC Proliferation and Differentiation Programs

To dissect the molecular pathways underlying delayed HFSC activation in *Sox4*-deficient skin, we performed microarray-based gene-expression profiling in telogen (resting) and anagen skin (Figures 5A, 5B, and S5A). Most of the differentially expressed genes (DEGs; false discovery rate [FDR] < 0.15) in telogen skin were related to immune response and cholesterol/hormone metabolism, as revealed by gene set enrichment analysis (GSEA; FDR < 0.05) and qPCR validation of some of these genes, such as *Defb8* or *Aoah* (Figures S5A–S5C; Table S2). Given that *Sox4* functions mainly as a transcriptional activator (van de Wetering et al., 1993) and its expression peaks during late onset of anagen, we then focused on the genes that were negatively regulated in $Sox4^{cKO}$ mice during plucking-induced anagen. A stringent analysis (FDR < 0.15) revealed 20 DEGs between $Sox4^{WT}$ and $Sox4^{cKO}$ mouse skin undergoing hair regeneration (Figure 5B; Table S3). Among them, *Sox4* was the most downregulated gene ($\log_2$FC = 4.9; 30-fold decrease) (Figure 5B; Table S3). We validated this by qPCR on some of the DEGs, including Tead2, *Mex3a*, *Tes*, *Evl*, and *Zfp184*, all of which are known *Sox4* targets (Bhattaram et al., 2010; Figure 5C). Most of these DEGs are involved in nervous system development, heart function, cytoskeleton remodeling, and cancer, as determined by Gene Ontology (GO) studies (Table S3). All these processes have been previously linked to *Sox4* (Vervoort et al., 2013) and therefore provided an additional biologically relevant quality control for our microarray.

Next, we performed GSEA during plucking to gain insights into the biological significance of these DEGs. GSEA revealed a significant alteration (FDR < 0.05) of 86 signaling pathways (extracted from the KEGG, Reactome, and NCI repositories) in $Sox4^{WT}$ versus $Sox4^{cKO}$ mice (Table S4). We confirmed a *Sox4* signature in the anagen microarray by analyzing genes identified by Liao et al. (2008) as an additional quality control (Figures 5D and S5D; FDR = 2.6×10^{-03}). In addition, we also observed very little overlap among the pathways that were significantly downregulated in the absence of Sox4 in telogen versus anagen (Figure 5E), thus reinforcing the specific role of Sox4 during the telogen-to-anagen transition, when the HFSC become activated (Lien et al., 2014). The gene sets that were downregulated in anagen $Sox4^{cKO}$ skin were mostly related to cell cycle, HFSC activation, and DNA repair (Figures 5F and 5G; Table S4). These included critical mitotic regulators such as *CDK4*, *Bub1*, and *Ccne1*, and genes of the DNA replication origin assembly such as *Rcf3*, *Mcm7*, and *Mcm10* (Figures 5F and 5G). We also found downregulation of DNA repair and replicative stress pathways in $Sox4^{cKO}$ mice undergoing hair regeneration, in agreement with a role for Sox4 in the DNA-damage response (Chetty et al., 2012; Figures 5F and 5G). Interestingly, several of the gene sets that were significantly downregulated in the absence of *Sox4* have been shown to be crucial for proper HF cycling and activation/differentiation of HFSCs (Berta et al., 2010; Lien et al., 2014; Nowak et al., 2008; Oro and Higgins, 2003). In particular, we found downregulation in the Myc and Shh pathways, in support of the previously shown delayed HFSC activation and wound repair (Figures 3C, 4I, 4J, 5F, and 5G). We further confirmed a defective HFSC function by testing a *Sox9*

signature from the Transfac repository. We observed a highly significant (FDR = 5.8 × 10^{-03}) downregulation of the Sox9 signature in *Sox4* ^{cKO} mice undergoing anagen compared with *Sox4* ^{WT} controls (Figures 5D and S5D). We used the *Sox5* signature as a negative control because it did not show significant variation in our microarray (Figures 5D and S6A). Finally, we compared our microarray data with the plucking-induced, Wnt-upregulated, *Ctnnb1*-sensitive gene signature obtained by Lien et al. (2014), a bona fide set of genes that govern HFSC activation during plucking. Interestingly, we found a significant downregulation of this set of genes (FDR < 1 × 10^{-03}) in Sox4-depleted skin 12 days after plucking compared with their WT controls (Figures 5F and 5G). We further validated most of these targets, such as *Gli1*, *Tcf7*, *Plk1*, and *Chk2*, by qPCR (Figure 5H). Importantly, most of these genes were not differentially regulated in telogen *Sox4* ^{cKO} skin (Figures S5E and S5F). This gene regulation exerted by Wnt/*Ctnnb1* and modulated by Sox4, which is exclusively restricted to activated skin, points to a cooperation between *Ctnnb1* and Sox4 in controlling target genes that are relevant for HFSC activation during normal hair regeneration.

Altogether, these results demonstrate that the absence of *Sox4* in skin results in delayed HFSC activation and subsequent deficient induction of proliferation and differentiation pathways concomitantly with defects in DNA damage repair, indicating that Sox4 is a crucial modulator of pathways that control the exit of HFSC quiescence.

Sox4 Deficiency Prevents Chemically Induced Skin Carcinogenesis

We have shown cancer resistance in hypomorphic *Sox4* $^{lox/lox}$ mice. Moreover, *Sox4*-deficient skin is resistant to HFSC activation, and several of the *Sox4*-regulated genes in our anagen microarray are related to cell-cycle regulation. In addition, *Sox4* is one of the most commonly upregulated genes in most cancer types and is required for induction of proliferative and cellsurvival pathways (Vervoort et al., 2013). As the next step in our study, we performed in vitro transformation protocols in order to assess Sox4 dependency during cellular transformation in mouse embryonic fibroblasts (MEFs). First, we assayed *Sox4* $^{lox/lox}$ and *Sox4* $^{+/+}$ MEFs previously transduced with Adeno-*Cre* viruses to induce recombination of the KI allele (hereafter termed *Sox4* $^{lox/lox}$; AdCre and *Sox4* $^{+/+}$; AdCre MEFs, respectively). We transduced the cells with *HRas* ^{G12V} and *E1a* oncogenes and plated them in clonogenic conditions. *Sox4* $^{lox/lox}$; AdCre MEFs showed a dramatically reduced number of transformed foci compared with the *Sox4* $^{+/+}$ controls, indicative of reduced transformation abilities (Figure 6A). Given the reduced cancer incidence in Sox4 hypomorphic mice (Figure 1I), we wanted to study the impact of reduced Sox4 levels specifically in skin carcinogenesis. For this purpose, we performed a two-step, chemically induced carcinogenesis protocol. We treated the mice with a single dose of 7,12-dimethylbenz[α] anthracene (DMBA) and administered 12-O-tetradecanoylphorbol-13-acetate (TPA) twice weekly during 15 additional weeks in order to promote expansion of cells bearing oncogenic mutations induced by DMBA, most of which have been shown to selectively cluster in the Ras pathway (Abel et al., 2009). We monitored tumor burden once a week during a total of 35 weeks after the first DMBA administration (Figure 6B). Interestingly, we observed that the onset of tumors was delayed in *Sox4* ^{cKO} mice (Figure 6C). Moreover, the average number of tumors per mouse was notably reduced across the

duration of experiment (Figures 6C and 6D). Of note, most of the papillomas that appeared in *Sox4*^{cKO} mice regressed upon TPA withdrawal, whereas up to 30% of the tumors that formed in *Sox4*^{WT} became independent of TPA administration and progressed (Figures 6C and 6E). In addition, *Sox4*-depleted mice did not display any papilloma larger than 6 mm after 30 weeks of treatment, in contrast to more than 80% of *Sox4*^{WT} mice (Figure 6E).

We also studied carcinogenesis in *Sox4*^{cHET} and *Sox4* hypomorphic (*Sox4*$^{lox/lox}$) mice. We observed a good correlation between *Sox4* gene dosage and tumor burden, as assessed by the total number of tumors and the percentage of mice bearing big tumors (Figure 6E). The fact that *Sox4*^{cHET} mice showed no obvious global defects in weight, size, or lifespan, but displayed a reduced number of tumors during TPA/DMBA owing to heterozygous deletion of Sox4 specifically in the skin, reinforces the notion that Sox4 plays a role in chemically induced skin carcinogenesis.

Resistance to TPA-Induced Proliferation Limits the Skin Tumor Burden in the Absence of *Sox4*

We wanted to understand the mechanism by which Sox4 deletion could contribute to preventing carcinogenesis. Given that the papilloma burden in *Sox4*^{WT} mice peaked between 12 and 15 weeks after TPA/DMBA administration (Figure 6C), we decided to sacrifice a group of animals after 6 weeks of treatment for a histological examination of skin prior to the onset of tumors (Figures 6C and S6A). Interestingly, we found a strong reduction in the percentage of proliferating cells, as assessed by Ki67 staining, in the IFE of *Sox4*^{cKO} mice, in agreement with a role for Sox4 in modulating the proliferative response under various stresses, as previously shown for plucking and wounding (Figures S6B and S6C). Accordingly, these mice showed reduced epidermal thickening and reduced HF length, confirming that *Sox4* is needed for cell expansion upon mitogenic stimulation (Figure S6C). We also studied the levels and distribution of phosphorylated Histone-3 (P-H3) by IHC in equivalent regions of benign lesions from *Sox4*^{WT} and *Sox4*^{cKO} mice, as determined from the distribution of the loricrin and CK6 markers. We observed a notable reduction in the number of cells that were positive for P-H3. In addition, the majority of the P-H3-positive cells in *Sox4*^{cKO} mouse skin showed a dotted pattern, indicating G2 cell-cycle arrest (Goto et al., 1999; Figure S6D). These findings are in line with the defective activation and proliferation of HFSCs upon stimulation we observed through both IHC and microarray profiling, which included downregulation of many genes required for cell division. These results suggest that the downregulation of cellcycle genes upon loss of *Sox4* may contribute to reduced tumor formation associated with decreased Sox4 levels (Figure 6F).

Discussion

Sox4 is a transcriptional activator that regulates the differentiation and maturation of many cell types (Bhattaram et al., 2010; Billiard et al., 2003; Lefebvre et al., 2007; Lioubinski et al., 2003). In adults, *Sox4* expression is restricted to the proliferative female reproductive system, activated HFSCs and HG cells, differentiating hematopoietic and lymphoid compartments, and the CNS, suggesting that Sox4 is tightly controlled (Greco et al., 2009; Hunt and Clarke, 1999; Kobielak et al., 2007; Lien et al., 2014; Lowry et al., 2005; Vervoort

et al., 2013). Indeed, *Sox4* is abnormally expressed in human cancer, where it strongly correlates with poor prognosis and metastasis (Vervoort et al., 2013).

Here, we sought to address the role of *Sox4* in the adult organism. In particular, we generated hypomorphic *Sox4* mice with decreased *Sox4* expression levels in the whole organism. Reduced *Sox4* levels in these mice are likely due to decreased *Sox4* mRNA stability associated with alteration of the 3' UTR sequence of the *Sox4* KI cassette (Amrani et al., 2004). Decreased *Sox4* levels in these mice lead to an earlier onset of several age-related pathologies and reduced lifespan. We think the decreased bone mineral density found in $Sox4^{lox/lox}$ (hypomorphic) mice is remarkable. Reduced *Sox4* expression is associated with postmenopausal bone frailty in humans (Duncan et al., 2011; Jemtland et al., 2011). Moreover, $Sox4^{+/-}$ mice show decreased osteogenesis and increased osteoporosis (Nissen-Meyer et al., 2007), suggesting a role for Sox4 in regulating bone homeostasis. $Sox4^{lox/lox}$ mice also show increased cardiac malformations reminiscent of the developmental defects that arise during late embryogenesis in $Sox4^{-/-}$ embryos. The absence of embryonic lethality in $Sox4^{lox/lox}$ mice suggests that low Sox4 levels are sufficient to sustain full embryonic development, but insufficient to ensure proper adult tissue homeostasis (Schilham et al., 1996).

Interestingly, global downregulation of *Sox4* mRNA in $Sox4^{lox/lox}$ mice also resulted in reduced cancer incidence, providing genetic evidence for *Sox4*'s previously reported oncogenic activity and overexpression in cancer (Penzo-Meéndez, 2010; Vervoort et al., 2013). To confirm that cancer resistance in $Sox4^{lox/lox}$ mice was not a secondary effect of reduced lifespan, we generated mice conditionally deleted for *Sox4* in the skin ($Sox4^{cKO}$ mice). We confirmed that these mice are strongly resistant to skin transformation in a two-step carcinogenesis protocol. The reduced tumorigenesis in $Sox4^{cKO}$, $Sox4^{lox/lox}$, and $Sox4^{cHET}$ mice and decreased Ras-induced foci in $Sox4^{lox/lox}$ AdCre MEFs suggest that *Sox4* is required for cellular transformation and acts in a dose-dependent manner. This is likely to be mediated by the resistance of *Sox4* mice to respond to proliferation-inducing agents, as shown by Ki67 and P-H3 staining in TPA-treated skin, prior to the onset of tumorigenesis. Indeed, under proliferative cues (such as with TPA treatment or hair plucking), *Sox4*-deficient mice showed a much reduced epidermal thickness and HF length.

Sox4 is also relevant for normal HFSC activation. Upon plucking, the delayed HFSC activation in $Sox4^{cKO}$ mice resulted in a significant delay in hair regeneration, as shown by assessment of hair-coat regeneration dynamics, histology, and transcriptional profiling. In agreement with this finding, a recent report showing the contribution of mobilized *Sox4*-positive, activated HFSC/HG and hair progeny to E6/E7 oncoprotein activity suggested a link between HFSC activation and skin tumorigenesis orchestrated through *Sox4* expression (da Silva-Diz et al., 2013). In line with this, a recent report showed that *Sox2*, another member of the *Sox* superfamily, can also control skin tumorigenesis by modulating critical pathways related to tumor-initiating cancer stem cells, thus connecting cancer with derailed stemness. Interestingly, *Sox2* seem to be induced in response to TPA/DMBA and mutated Ras, in agreement with the behavior of *Sox4* in vitro and in vivo (Boumahdi et al., 2014). In support of a connection between *Sox2* and *Sox4*, it has been demonstrated that autocrine TGF-β-mediated induction of *Sox4* is critical for *Sox2* upregulation to confer malignancy

and stemness features to glioma-initiating cells (Ikushima et al., 2009). Remarkably, we identified several gene sets that were specifically downregulated in *Sox4*-depleted skin during anagen, indicating an important role for this protein during induction of the hair cycle. Notably, some of these pathways are related to cell cycle and DNA synthesis, which can account for an increased quiescence of HFSCs depleted of Sox4 and thus reduced expansion of these cell populations, in agreement with the observed longer telomeres in *Sox4*^{cKO} mice HFSC compartments. In this regard, a Wnt-dependent gene-expression signature that is activated through *Ctnnb1*-mediated relief of Tcf3/4 repression during hair plucking was elegantly elucidated in a recent study (Lien et al., 2014). Interestingly, we detected a significant downregulation of this *Ctnnb1*-sensitive signature in our microarray data in *Sox4*^{cKO} versus *Sox4*^{WT} skin specifically during the hair-plucking response. These results are indicative of an interplay between the cues that govern hair regeneration with Sox4-mediated transcription. Interestingly, when *Sox4*-depleted HFSCs were forced to proliferate upon plucking, they displayed increased DNA damage and reduced proliferation compared with their *Sox4*^{WT} littermates. This supports a role for Sox4 in HFSC activation and points to a function for Sox4 in alleviating different types of stress, as evidenced by increased γH2AX in cells depleted of Sox4 under proliferative conditions, in agreement with previous reports (Chetty et al., 2012). Finally, most of the DEGs in *Sox4*^{cKO} mice during plucking were linked to cancer, further supporting a resistance to expansion and proliferation of epidermal keratinocytes during both physiological and pathological HFSC activation in the absence of Sox4 protein.

Overall, our results highlight the crucial roles that Sox4 has in cancer and HFSC activation, and provide new avenues for elucidating the roles of this transcription factor in vivo.

Experimental Procedures

Mouse Experimentation

Mice were maintained at the Spanish National Cancer Research Center (CNIO) under pathogen-free conditions, following the recommendations of the Federation of European Laboratory Animal Science Associations (FELASA).

Generation of the *Sox4*-IRES-GFP/Luciferase (*Sox4*^{KI}) Mouse Model

Sox4^{KI} mice were generated by genOway. All mice used were of a mixed back-ground (C57BL6/129Sv, 75%:25%).

Histopathology and IHC

Histology and IHC were performed as described previously (Martínez et al., 2009) using the following antibodies and dilutions: mouse monoclonal anti-GFP (Roche, 1:500), rabbit polyclonal anti-CK14 (Covance, 1:1,000), rabbit polyclonal anti-CK10 (Covance, 1:300), rabbit polyclonal anti-Loricrin (Covance, 1:500), rabbit polyclonal anti-p53 (CM5 Novocastra, 1:200), mouse monoclonal anti-Ki67 (Master Diagnostica, 1:200), mouse monoclonal anti-Histone 3 phospho-Ser10 (Millipore, 1:200), mouse monoclonal anti-Histone 2 phospho-Ser139 (γH2AX, Millipore, 1:100), mouse monoclonal anti-p63 (Neo Markers, 1:100), and rat monoclonal anti-BrdU (Abcam, 1:50). Images were captured in a

bright-field microscope under 20× or 40× magnification and quantified using ImageJ. At least 500–1,000 nuclei per skin region and mouse were scored, and values were represented as the percentage of positive nuclei per mouse.

Molecular Imaging

Lean mass, fat content, and bone mineral density were analyzed by DEXA using a Lunar PIXImus Densitometer (GE Medical Systems) on mice anesthetized with 2% isoflurane. The acquisition time was 5 min. Bone mineral density was calculated from a region of interest (ROI) including the whole left femur.

Clonogenic Assays

Total keratinocytes from newborn or adult mice were isolated as described previously (Jensen et al., 2010). Cells were resuspended in Cnt-02 medium (CELLnTEC) and counted. Then 1×10^3 cells were seeded in triplicates onto 35 mm wells on top of MitomycinC-treated feeder layers in Cnt-02 medium and cultured for 2 weeks. The cells were then fixed in 10% formaldehyde (30 min at room temperature) and stained with Giemsa or rhodamine. Colonies were counted and measured with ImageJ from scanned images. Each mouse skin was plated in triplicate wells and averaged for individual mouse values, and data were represented as the average per mouse.

Microarray-Based Transcriptional Profiling

Total RNA from resting or plucked skin was extracted with the QIAGEN RNAlater and RNEasy Mini Kits. The RNA integrity number (RIN) was in the range of 7–9.8 according to the Agilent 2100 Bioanalyzer. Total RNA (100 ng) was labeled with the One-Color Microarray-Based Gene Expression Analysis (Low Input Quick Amp Labeling) kit (version 6.5; Agilent Technologies) and purified with silica-based spin columns (BioRad). Hybridization and analysis were performed as described previously (MartÍnez et al., 2013).

Supplemental Information

Refer to Web version on PubMed Central for supplementary material.

Acknowledgments

We are indebted to R. Serrano and E. Collado for animal care; L. Morgado, L. Martínez, and D. Megías for advice; and G. Luengo and O. DomÍnguez for microarray hybridization. M.F. is funded by the Spanish Ministry of Education. M.A.B.'s laboratory is funded by ERC Project TEL STEM CELL (GA#232854), EU FP7 Projects 2007-A-20088 (MARK-AGE) and 2010-259749 (EuroBATS), Spanish Ministry of Economy and Competitiveness Projects SAF2008-05384 and CSD2007-00017, Government of Madrid Project S2010/BMD-2303 (ReCaRe), the AXA Research Fund (Life Risks Project), and the Fundacion Botín (Spain).

References

Abel EL, Angel JM, Kiguchi K, DiGiovanni J. Multi-stage chemical carcinogenesis in mouse skin: fundamentals and applications. Nat Protoc. 2009; 4:1350–1362. [PubMed: 19713956]

Alonso L, Fuchs E. The hair cycle. J Cell Sci. 2006; 119:391–393. [PubMed: 16443746]

Amrani N, Ganesan R, Kervestin S, Mangus DA, Ghosh S, Jacobson A. A faux 3'-UTR promotes aberrant termination and triggers nonsense-mediated mRNA decay. Nature. 2004; 432:112–118. [PubMed: 15525991]

Aue G, Du Y, Cleveland SM, Smith SB, Davé UP, Liu D, Weniger MA, Metais JY, Jenkins NA, Copeland NG, Dunbar CE. Sox4 cooperates with PU.1 haploinsufficiency in murine myeloid leukemia. Blood. 2011; 118:4674–4681. [PubMed: 21878674]

Berta MA, Baker CM, Cottle DL, Watt FM. Dose and context dependent effects of Myc on epidermal stem cell proliferation and differentiation. EMBO Mol Med. 2010; 2:16–25. [PubMed: 20043278]

Bhattaram P, Penzo-Méndez A, Sock E, Colmenares C, Kaneko KJ, Vassilev A, Depamphilis ML, Wegner M, Lefebvre V. Organogenesis relies on SoxC transcription factors for the survival of neural and mesenchymal progenitors. Nat Commun. 2010; 1:9. [PubMed: 20596238]

Billiard J, Moran RA, Whitley MZ, Chatterjee-Kishore M, Gillis K, Brown EL, Komm BS, Bodine PV. Transcriptional profiling of human osteoblast differentiation. J Cell. Biochem. 2003; 89:389–400. [PubMed: 12704802]

Blanco S, Kurowski A, Nichols J, Watt FM, Benitah SA, Frye M. The RNA-methyltransferase Misu (NSun2) poises epidermal stem cells to differentiate. PLoS Genet. 2011; 7:e1002403. [PubMed: 22144916]

Blanpain C, Fuchs E. Epidermal homeostasis: a balancing act of stem cells in the skin. Nat Rev Mol Cell Biol. 2009; 10:207–217. [PubMed: 19209183]

Boumahdi S, Driessens G, Lapouge G, Rorive S, Nassar D, Le Mercier M, Delatte B, Caauwe A, Lenglez S, Nkusi E, et al. SOX2 controls tumour initiation and cancer stem-cell functions in squamous-cell carcinoma. Nature. 2014; doi: 10.1038/nature13305

Boyd KE, Xiao YY, Fan K, Poholek A, Copeland NG, Jenkins NA, Perkins AS. Sox4 cooperates with Evi1 in AKXD-23 myeloid tumors via transactivation of proviral LTR. Blood. 2006; 107:733–741. [PubMed: 16204320]

Braun KM, Niemann C, Jensen UB, Sundberg JP, Silva-Vargas V, Watt FM. Manipulation of stem cell proliferation and lineage commitment: visualisation of label-retaining cells in wholemounts of mouse epidermis. Development. 2003; 130:5241–5255. [PubMed: 12954714]

Canela A, Vera E, Klatt P, Blasco MA. High-throughput telomere length quantification by FISH and its application to human population studies. Proc Natl Acad Sci USA. 2007; 104:5300–5305. [PubMed: 17369361]

Chetty C, Dontula R, Gujrati M, Dinh DH, Lakka SS. Blockade of SOX4 mediated DNA repair by SPARC enhances radioresponse in medulloblastoma. Cancer Lett. 2012; 323:188–198. [PubMed: 22542805]

da Silva-Diz V, Solé-Sánchez S, Valdés-Gutiérrez A, Urpí M, Riba-Artés D, Penin RM, Pascual G, González-Suárez E, Casanovas O, Viñals F, et al. Progeny of Lgr5-expressing hair follicle stem cell contributes to papillomavirus-induced tumor development in epidermis. Oncogene. 2013; 32:3732–3743. [PubMed: 22945646]

de Jesus BB, Blasco MA. Assessing cell and organ senescence biomarkers. Circ Res. 2012; 111:97–109. [PubMed: 22723221]

Deneault E, Cellot S, Faubert A, Laverdure JP, Fréchette M, Chagraoui J, Mayotte N, Sauvageau M, Ting SB, Sauvageau G. A functional screen to identify novel effectors of hematopoietic stem cell activity. Cell. 2009; 137:369–379. [PubMed: 19379700]

Du Y, Spence SE, Jenkins NA, Copeland NG. Cooperating cancer-gene identification through oncogenic-retrovirus-induced insertional mutagenesis. Blood. 2005; 106:2498–2505. [PubMed: 15961513]

Duncan EL, Danoy P, Kemp JP, Leo PJ, McCloskey E, Nicholson GC, Eastell R, Prince RL, Eisman JA, Jones G, et al. Genome-wide association study using extreme truncate selection identifies novel genes affecting bone mineral density and fracture risk. PLoS Genet. 2011; 7:e1001372. [PubMed: 21533022]

Dy P, Penzo-Méndez A, Wang H, Pedraza CE, Macklin WB, Lefebvre V. The three SoxC proteins—Sox4, Sox11 and Sox12— exhibit overlapping expression patterns and molecular properties. Nucleic Acids Res. 2008; 36:3101–3117. [PubMed: 18403418]

Flores I, Cayuela ML, Blasco MA. Effects of telomerase and telomere length on epidermal stem cell behavior. Science. 2005; 309:1253–1256. [PubMed: 16037417]

Flores I, Canela A, Vera E, Tejera A, Cotsarelis G, Blasco MA. The longest telomeres: a general signature of adult stem cell compartments. Genes Dev. 2008; 22:654–667. [PubMed: 18283121]

Fuchs E. Epidermal differentiation and keratin gene expression. Int Symp Princess Takamatsu Cancer Res Fund. 1994; 24:290–302. [PubMed: 8983083]

Fuchs E. Scratching the surface of skin development. Nature. 2007; 445:834–842. [PubMed: 17314969]

Fuchs E. The tortoise and the hair: slow-cycling cells in the stem cell race. Cell. 2009; 137:811–819. [PubMed: 19490891]

Garinis GA, van der Horst GT, Vijg J, Hoeijmakers JH. DNA damage and ageing: new-age ideas for an age-old problem. Nat Cell Biol. 2008; 10:1241–1247. [PubMed: 18978832]

Goto H, Tomono Y, Ajiro K, Kosako H, Fujita M, Sakurai M, Okawa K, Iwamatsu A, Okigaki T, Takahashi T, Inagaki M. Identification of a novel phosphorylation site on histone H3 coupled with mitotic chromosome condensation. J Biol Chem. 1999; 274:25543–25549. [PubMed: 10464286]

Greco V, Chen T, Rendl M, Schober M, Pasolli HA, Stokes N, Dela Cruz-Racelis J, Fuchs E. A two-step mechanism for stem cell activation during hair regeneration. Cell Stem Cell. 2009; 4:155–169. [PubMed: 19200804]

Harley V, Lefebvre V. Twenty Sox, twenty years. Int J Biochem Cell Biol. 2010; 42:376–377. [PubMed: 20004736]

Hoeijmakers JH. DNA damage, aging, and cancer. N Engl J Med. 2009; 361:1475–1485. [PubMed: 19812404]

Hoser M, Potzner MR, Koch JM, Bösl MR, Wegner M, Sock E. Sox12 deletion in the mouse reveals nonreciprocal redundancy with the related Sox4 and Sox11 transcription factors. Mol Cell Biol. 2008; 28:4675–4687. [PubMed: 18505825]

Hsu YC, Pasolli HA, Fuchs E. Dynamics between stem cells, niche, and progeny in the hair follicle. Cell. 2011; 144:92–105. [PubMed: 21215372]

Huang J, Arsenault M, Kann M, Lopez-Mendez C, Saleh M, Wadowska D, Taglienti M, Ho J, Miao Y, Sims D, et al. The transcription factor Sry-related HMG box-4 (SOX4) is required for normal renal development in vivo. Dev Dyn. 2013; 242:790–799. [PubMed: 23559562]

Hunt SM, Clarke CL. Expression and hormonal regulation of the Sox4 gene in mouse female reproductive tissues. Biol Reprod. 1999; 61:476–481. [PubMed: 10411530]

Hur W, Rhim H, Jung CK, Kim JD, Bae SH, Jang JW, Yang JM, Oh ST, Kim DG, Wang HJ, et al. SOX4 overexpression regulates the p53-mediated apoptosis in hepatocellular carcinoma: clinical implication and functional analysis in vitro. Carcinogenesis. 2010; 31:1298–1307. [PubMed: 20400479]

Ikushima H, Todo T, Ino Y, Takahashi M, Miyazawa K, Miyazono K. Autocrine TGF-beta signaling maintains tumorigenicity of glioma-initiating cells through Sry-related HMG-box factors. Cell Stem Cell. 2009; 5:504–514. [PubMed: 19896441]

Jafarnejad SM, Ardekani GS, Ghaffari M, Li G. Pleiotropic function of SRY-related HMG box transcription factor 4 in regulation of tumorigenesis. Cell Mol Life Sci. 2013; 70:2677–2696. [PubMed: 23080209]

Jaks V, Barker N, Kasper M, van Es JH, Snippert HJ, Clevers H, Toftgård R. Lgr5 marks cycling, yet long-lived, hair follicle stem cells. Nat Genet. 2008; 40:1291–1299. [PubMed: 18849992]

Jemtland R, Holden M, Reppe S, Olstad OK, Reinholt FP, Gautvik VT, Refvem H, Frigessi A, Houston B, Gautvik KM. Molecular disease map of bone characterizing the postmenopausal osteoporosis phenotype. J Bone Miner Res. 2011; 26:1793–1801. [PubMed: 21452281]

Jensen KB, Collins CA, Nascimento E, Tan DW, Frye M, Itami S, Watt FM. Lrig1 expression defines a distinct multipotent stem cell population in mammalian epidermis. Cell Stem Cell. 2009; 4:427–439. [PubMed: 19427292]

Jensen KB, Driskell RR, Watt FM. Assaying proliferation and differentiation capacity of stem cells using disaggregated adult mouse epidermis. Nat Protoc. 2010; 5:898–911. [PubMed: 20431535]

Keyes BE, Segal JP, Heller E, Lien WH, Chang CY, Guo X, Oristian DS, Zheng D, Fuchs E. Nfatc1 orchestrates aging in hair follicle stem cells. Proc Natl Acad Sci USA. 2013; 110:E4950–E4959. [PubMed: 24282298]

Kobielak K, Stokes N, de la Cruz J, Polak L, Fuchs E. Loss of a quiescent niche but not follicle stem cells in the absence of bone morphogenetic protein signaling. Proc Natl Acad Sci USA. 2007; 104:10063–10068. [PubMed: 17553962]

Kuwahara M, Yamashita M, Shinoda K, Tofukuji S, Onodera A, Shinnakasu R, Motohashi S, Hosokawa H, Tumes D, Iwamura C, et al. The transcription factor Sox4 is a downstream target of signaling by the cytokine TGF-β and suppresses T(H)2 differentiation. Nat Immunol. 2012; 13:778–786. [PubMed: 22751141]

Lefebvre V, Dumitriu B, Penzo-Méndez A, Han Y, Pallavi B. Control of cell fate and differentiation by Sry-related high-mobility-group box (Sox) transcription factors. Int J Biochem Cell Biol. 2007; 39:2195–2214. [PubMed: 17625949]

Li Z, Kustikova OS, Kamino K, Neumann T, Rhein M, Grassman E, Fehse B, Baum C. Insertional mutagenesis by replication-deficient retroviral vectors encoding the large T oncogene. Ann N Y Acad Sci. 2007; 1106:95–113. [PubMed: 17395733]

Liao YL, Sun YM, Chau GY, Chau YP, Lai TC, Wang JL, Horng JT, Hsiao M, Tsou AP. Identification of SOX4 target genes using phylogenetic footprinting-based prediction from expression microarrays suggests that overexpression of SOX4 potentiates metastasis in hepatocellular carcinoma. Oncogene. 2008; 27:5578–5589. [PubMed: 18504433]

Lien WH, Polak L, Lin M, Lay K, Zheng D, Fuchs E. In vivo transcriptional governance of hair follicle stem cells by canonical Wnt regulators. Nat Cell Biol. 2014; 16:179–190. [PubMed: 24463605]

Lioubinski O, Müller M, Wegner M, Sander M. Expression of Sox transcription factors in the developing mouse pancreas. Dev Dyn. 2003; 227:402–408. [PubMed: 12815626]

López-Otín C, Blasco MA, Partridge L, Serrano M, Kroemer G. The hallmarks of aging. Cell. 2013; 153:1194–1217. [PubMed: 23746838]

Lowry WE, Blanpain C, Nowak JA, Guasch G, Lewis L, Fuchs E. Defining the impact of beta-catenin/Tcf transactivation on epithelial stem cells. Genes Dev. 2005; 19:1596–1611. [PubMed: 15961525]

Martínez P, Thanasoula M, Muñoz P, Liao C, Tejera A, McNees C, Flores JM, Fernández-Capetillo O, Tarsounas M, Blasco MA. Increased telomere fragility and fusions resulting from TRF1 deficiency lead to degenerative pathologies and increased cancer in mice. Genes Dev. 2009; 23:2060–2075. [PubMed: 19679647]

Martínez P, Gómez-López G, García F, Mercken E, Mitchell S, Flores JM, de Cabo R, Blasco MA. RAP1 protects from obesity through its extratelomeric role regulating gene expression. Cell Reports. 2013; 3:2059–2074. [PubMed: 23791526]

Müller-Röver S, Handjiski B, van der Veen C, Eichmüller S, Foitzik K, McKay IA, Stenn KS, Paus R. A comprehensive guide for the accurate classification of murine hair follicles in distinct hair cycle stages. J Invest Dermatol. 2001; 117:3–15. [PubMed: 11442744]

Nissen-Meyer LS, Jemtland R, Gautvik VT, Pedersen ME, Paro R, Fortunati D, Pierroz DD, Stadelmann VA, Reppe S, Reinholt FP, et al. Osteopenia, decreased bone formation and impaired osteoblast development in Sox4 heterozygous mice. J Cell Sci. 2007; 120:2785–2795. [PubMed: 17652162]

Nowak JA, Polak L, Pasolli HA, Fuchs E. Hair follicle stem cells are specified and function in early skin morphogenesis. Cell Stem Cell. 2008; 3:33–43. [PubMed: 18593557]

Omidvar N, Maunakea ML, Jones L, Sevcikova S, Yin B, Himmel KL, Tennant TR, Le Beau MM, Largaespada DA, Kogan SC. PML-RARα co-operates with Sox4 in acute myeloid leukemia development in mice. Haematologica. 2013; 98:424–427. [PubMed: 23144197]

Oro AE, Higgins K. Hair cycle regulation of Hedgehog signal reception. Dev Biol. 2003; 255:238–248. [PubMed: 12648487]

Oshimori N, Fuchs E. The harmonies played by TGF-β in stem cell biology. Cell Stem Cell. 2012; 11:751–764. [PubMed: 23217421]

Parvani JG, Schiemann WP. Sox4, EMT programs, and the metastatic progression of breast cancers: mastering the masters of EMT. Breast Cancer Res. 2013; 15:R72. [PubMed: 23981787]

Penzo-Méndez AI. Critical roles for SoxC transcription factors in development and cancer. Int J Biochem Cell Biol. 2010; 42:425–428. [PubMed: 19651233]

Ramirez A, Page A, Gandarillas A, Zanet J, Pibre S, Vidal M, Tusell L, Genesca A, Whitaker DA, Melton DW, Jorcano JL. A keratin K5Cre transgenic line appropriate for tissue-specific or generalized Cre-mediated recombination. Genesis. 2004; 39:52–57. [PubMed: 15124227]

Rendl M, Polak L, Fuchs E. BMP signaling in dermal papilla cells is required for their hair follicle-inductive properties. Genes Dev. 2008; 22:543–557. [PubMed: 18281466]

Rhee H, Polak L, Fuchs E. Lhx2 maintains stem cell character in hair follicles. Science. 2006; 312:1946–1949. [PubMed: 16809539]

Sandoval S, Kraus C, Cho EC, Cho M, Bies J, Manara E, Accordi B, Landaw EM, Wolff L, Pigazzi M, Sakamoto KM. Sox4 cooperates with CREB in myeloid transformation. Blood. 2012; 120:155–165. [PubMed: 22627767]

Schilham MW, Oosterwegel MA, Moerer P, Ya J, de Boer PA, van de Wetering M, Verbeek S, Lamers WH, Kruisbeek AM, Cumano A, Clevers H. Defects in cardiac outflow tract formation and pro-Blymphocyte expansion in mice lacking Sox-4. Nature. 1996; 380:711–714. [PubMed: 8614465]

Schilham MW, Moerer P, Cumano A, Clevers HC. Sox-4 facilitates thymocyte differentiation. Eur J Immunol. 1997; 27:1292–1295. [PubMed: 9174623]

Sharpless NE, DePinho RA. How stem cells age and why this makes us grow old. Nat Rev Mol Cell Biol. 2007; 8:703–713. [PubMed: 17717515]

Shin MS, Fredrickson TN, Hartley JW, Suzuki T, Akagi K, Morse HC 3rd. High-throughput retroviral tagging for identification of genes involved in initiation and progression of mouse splenic marginal zone lymphomas. Cancer Res. 2004; 64:4419–4427. [PubMed: 15231650]

Snippert HJ, Haegebarth A, Kasper M, Jaks V, van Es JH, Barker N, van de Wetering M, van den Born M, Begthel H, Vries RG, et al. Lgr6 marks stem cells in the hair follicle that generate all cell lineages of the skin. Science. 2010; 327:1385–1389. [PubMed: 20223988]

Solanas G, Benitah SA. Regenerating the skin: a task for the heterogeneous stem cell pool and surrounding niche. Nat Rev Mol Cell Biol. 2013; 14:737–748. [PubMed: 24064540]

Sun B, Mallampati S, Gong Y, Wang D, Lefebvre V, Sun X. Sox4 is required for the survival of pro-B cells. J Immunol. 2013; 190:2080–2089. [PubMed: 23345330]

Tavazoie SF, Alarcón C, Oskarsson T, Padua D, Wang Q, Bos PD, Gerald WL, Massagué J. Endogenous human microRNAs that suppress breast cancer metastasis. Nature. 2008; 451:147–152. [PubMed: 18185580]

Tiwari N, Tiwari VK, Waldmeier L, Balwierz PJ, Arnold P, Pachkov M, Meyer-Schaller N, Schübeler D, van Nimwegen E, Christofori G. Sox4 is a master regulator of epithelial-mesenchymal transition by controlling Ezh2 expression and epigenetic reprogramming. Cancer Cell. 2013; 23:768–783. [PubMed: 23764001]

van de Wetering M, Oosterwegel M, van Norren K, Clevers H. Sox-4, an Sry-like HMG box protein, is a transcriptional activator in lymphocytes. EMBO J. 1993; 12:3847–3854. [PubMed: 8404853]

Van der Flier LG, Sabates-Bellver J, Oving I, Haegebarth A, De Palo M, Anti M, Van Gijn ME, Suijkerbuijk S, Van de Wetering M, Marra G, Clevers H. The Intestinal Wnt/TCF Signature. Gastroenterology. 2007; 132:628–632. [PubMed: 17320548]

Vera E, Bernardes de Jesus B, Foronda M, Flores JM, Blasco MA. The rate of increase of short telomeres predicts longevity in mammals. Cell Reports. 2012; 2:732–737. [PubMed: 23022483]

Vervoort SJ, van Boxtel R, Coffer PJ. The role of SRY-related HMG box transcription factor 4 (SOX4) in tumorigenesis and metastasis: friend or foe? Oncogene. 2013; 32:3397–3409. [PubMed: 23246969]

Watt FM. Stem cell fate and patterning in mammalian epidermis. Curr Opin Genet Dev. 2001; 11:410–417. [PubMed: 11448627]

Wilson ME, Yang KY, Kalousova A, Lau J, Kosaka Y, Lynn FC, Wang J, Mrejen C, Episkopou V, Clevers HC, German MS. The HMG box transcription factor Sox4 contributes to the development of the endocrine pancreas. Diabetes. 2005; 54:3402–3409. [PubMed: 16306355]

Zhang H, Alberich-Jorda M, Amabile G, Yang H, Staber PB, Di Ruscio A, Welner RS, Ebralidze A, Zhang J, Levantini E, et al. Sox4 is a key oncogenic target in C/EBPα mutant acute myeloid leukemia. Cancer Cell. 2013; 24:575–588. [PubMed: 24183681]

Europe PMC Funders Author Manuscripts

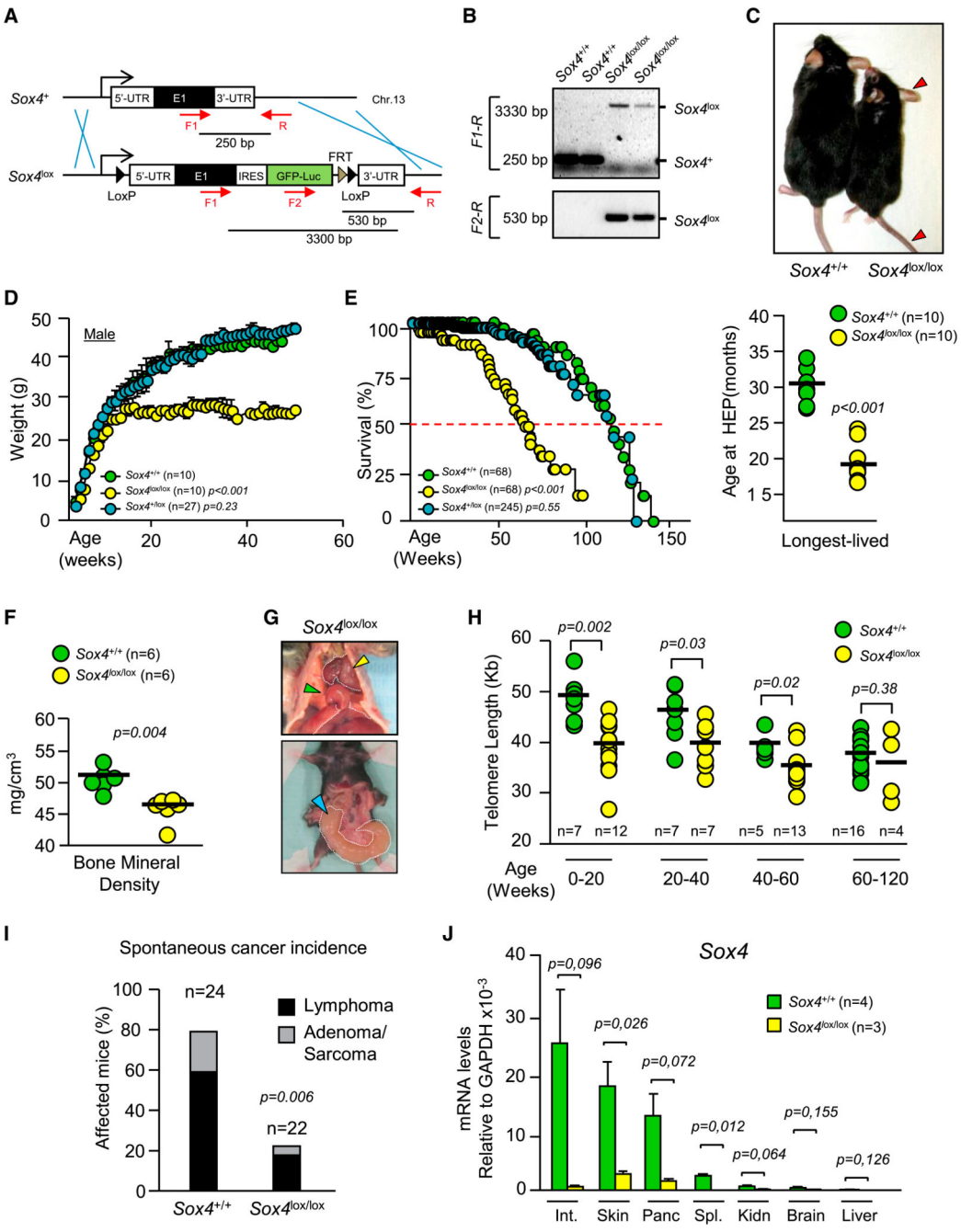

Figure 1. *Sox4*$^{lox/lox}$ Mice Display Cancer Resistance and Accelerated Aging

(A) Schematic representation of the different *Sox4* alleles. The genotyping primers (red arrows) and PCR sizes in base pairs (bp) are depicted.

(B) Genotyping PCR of the different *Sox4* alleles.

(C) Macroscopic aspect of *Sox4*$^{+/+}$ and *Sox4*$^{lox/lox}$ mice. Increased pigmentation in exposed skin is indicated by red arrowheads.

(D) Body weight of mice of the indicated genotypes.

(E) Left: Kaplan-Meyer survival curves; p values refer to comparison with *Sox4*$^{+/+}$ mice (log rank test). Dashed red line indicates mean lifespan. Right: lifespan of the ten longest-lived mice of the indicated genotype.
(F) Bone mineral density (BMD) of *Sox4*$^{+/+}$ and *Sox4*$^{lox/lox}$ mice.
(G) Representative images of *Sox4*$^{lox/lox}$ mice at the HEP. Green arrowhead marks congenital diaphragmatic hernia, yellow arrowhead indicates dilated cardiomyopathy, and blue arrowhead points to pyometra.
(H) High-throughput QFISH in mice of the indicated age and genotype.
(I) Spontaneous cancer incidence in the indicated genotypes. Fisher's exact test was used for comparison.
(J) qPCR of *Sox4* mRNA in the indicated tissues of *Sox4*$^{+/+}$ and *Sox4*$^{lox/lox}$ mice.
The p values and number of mice per genotype (n) are indicated (two-tailed Student's t test was used unless specified otherwise). Bars depict average values, error bars are SEM.
See also Figures S1 and S2, and Tables S1 and S5.

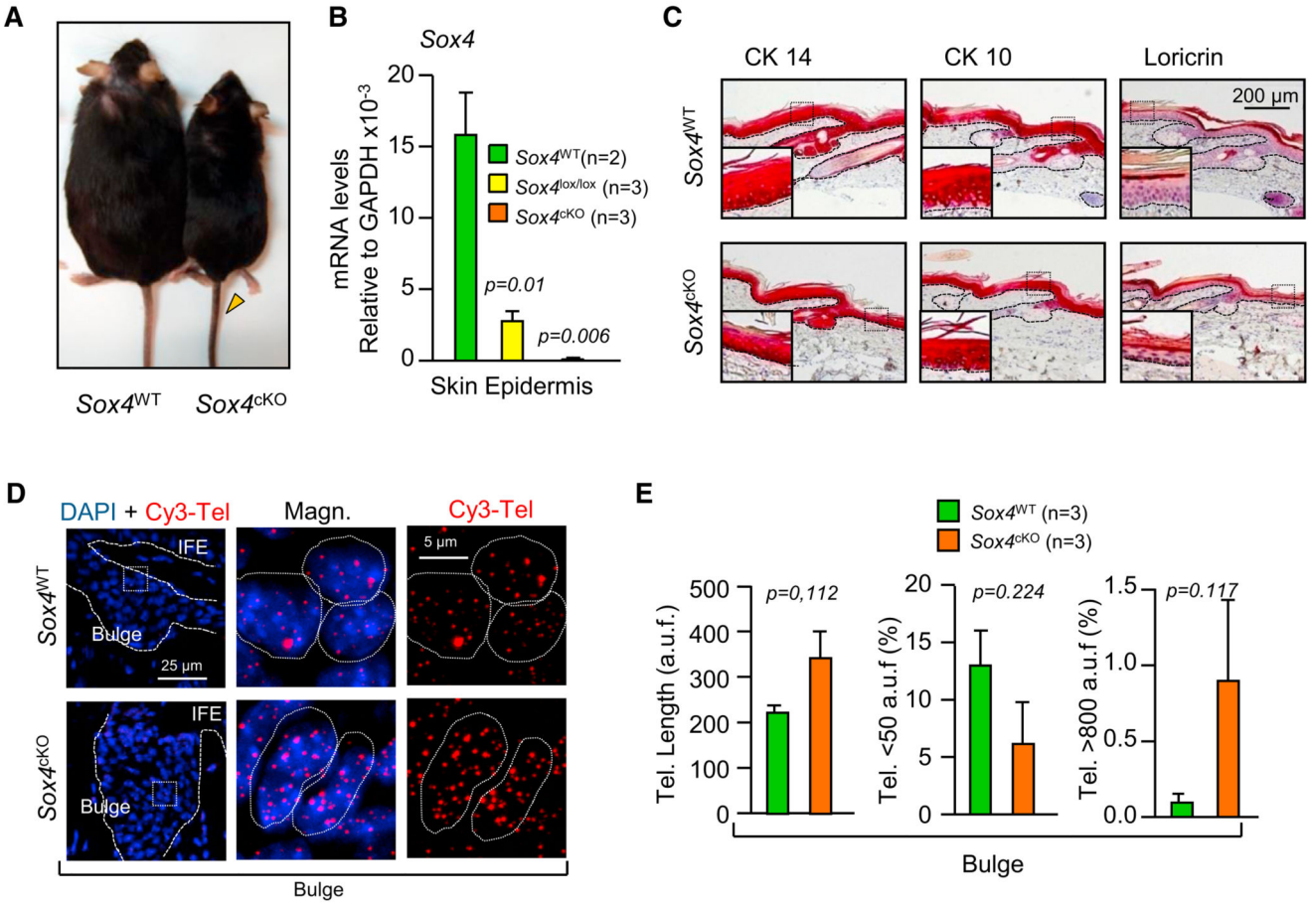

Figure 2. Normal Skin Stratification in the Absence of Sox4 and Reduced Replicative History in *Sox4*^{cKO} Bulge Cells

(A) *Sox4*^{WT} and *Sox4*^{cKO} mice at 6 months of age. Orange arrowheads mark hyperpigmentation.

(B) *Sox4* qPCR in skin epidermis of the indicated genotypes.

(C) IHC for CK14, CK10, and loricrin in tail skin sections from adult *Sox4*^{WT} and *Sox4*^{cKO} mice. Insets depict magnification. The images are representative of five mice per genotype.

(D) QFISH on the tail skin (bulge region) of an adult mouse (6 months old). The IFE and bulge are indicated in the images (middle panels: magnification [Magn.]).

(E) Mean telomere length (left panel), percentage of short telomeres (middle panel), and long telomeres (right panel) from the bulge region. n, number of analyzed mice per genotype; error is SEM; p values are indicated (two-tailed Student's t test). Scale bars are depicted in graphs.

See also Figure S3.

Europe PMC Funders Author Manuscripts

Europe PMC Funders Author Manuscripts

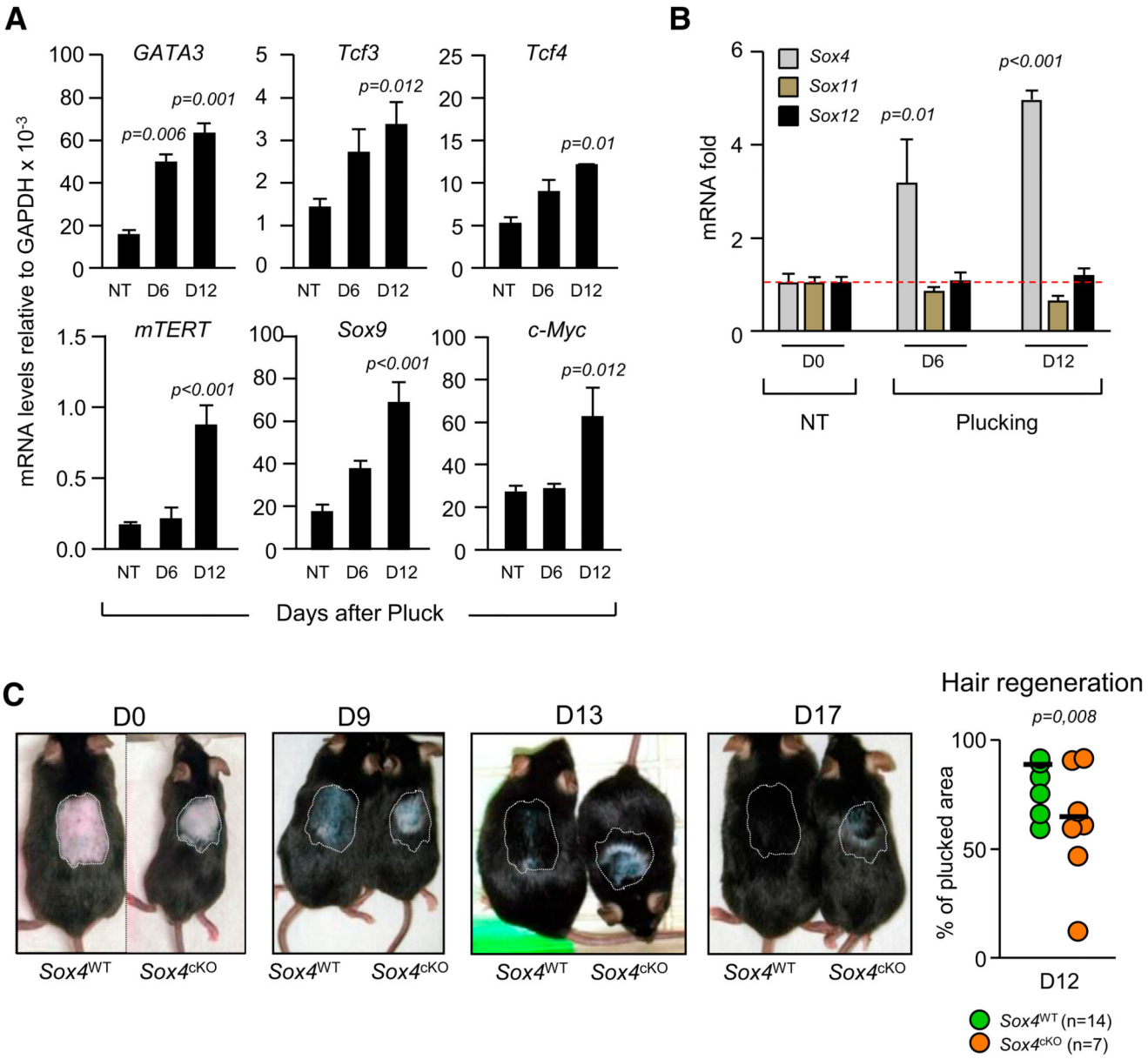

Figure 3. *Sox4* Is Induced after Hair Plucking and Is Required for Normal Hair Regeneration

(A) qPCR analysis of the indicated genes (NT, non-treated; mid and late anagen, D6 and D12, respectively) in WT mice. Two to three mice per condition were analyzed.

(B) *Sox4*, *Sox11*, and *Sox12* qPCR during plucking-induced anagen. n = 2–3 mice per condition. Depicted is fold over NT.

(C) Left: hair regeneration dynamics in $Sox4^{WT}$ and $Sox4^{cKO}$ mice. The initial plucking area is delineated by white dashed lines. Right: quantification of hair regeneration at D12 after plucking as the means of the regenerated area (%) with respect to that of the initial plucked area. The genotype and number (n) of mice are shown; p values were obtained by Student's t test; mean and SEM are depicted. See also Figure S4.

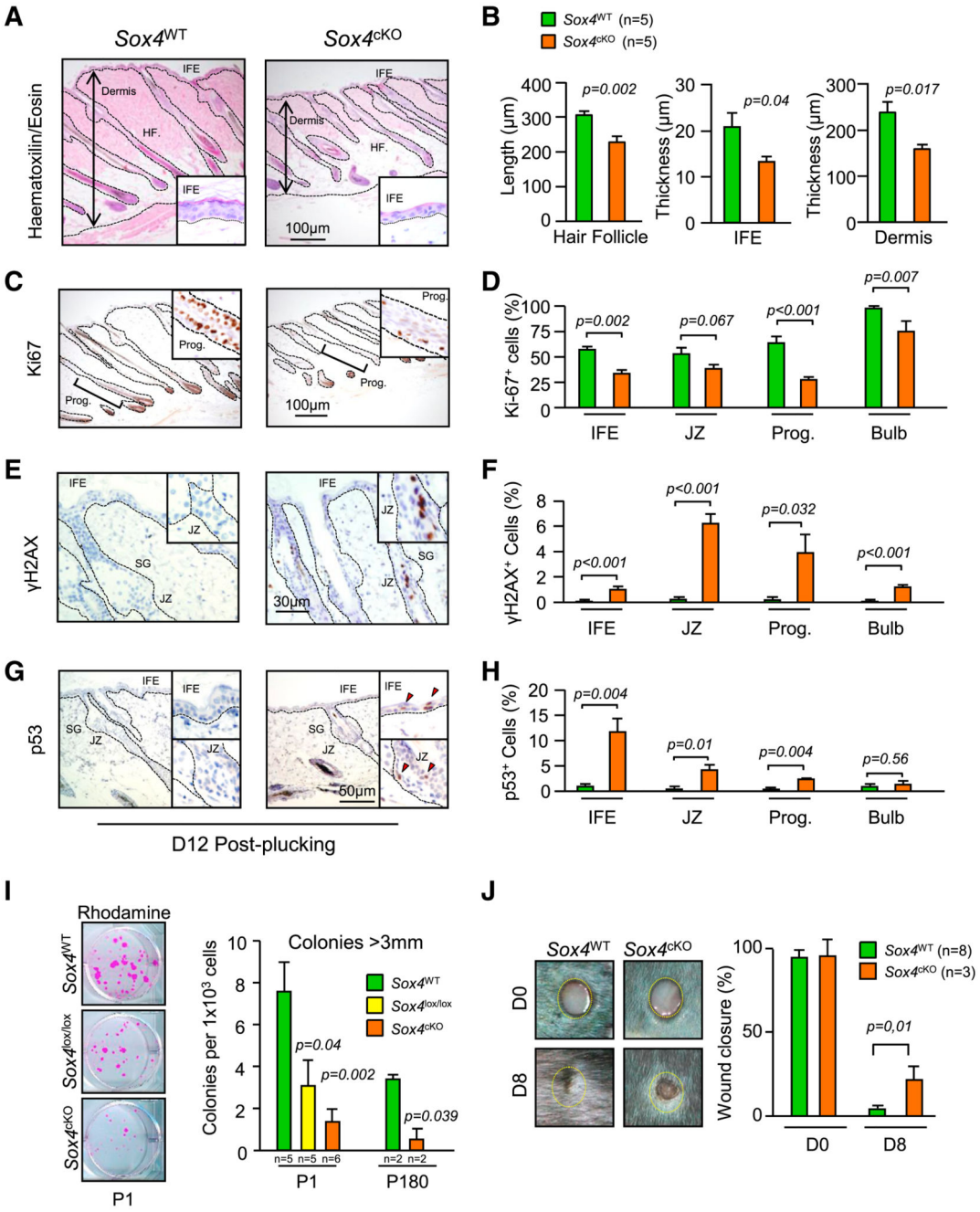

Figure 4. *Sox4* Is Required for Normal HFSC Activation during Hair Regeneration and Wound Healing

(A) Hematoxylin and eosin staining in *Sox4*^{WT} and *Sox4*^{cKO} mouse back skin sections at D12 after plucking. Skin regions are delineated by dashed lines.

(B) HF length, epidermis thickness, and dermal size from the experiment described in (A).

(C–H) Left: Ki67 (C), γH2AX (E), and p53 (G) IHCs on back skin sections from *Sox4*^{WT} and *Sox4*^{cKO} mice at D12 after plucking. Insets show magnification. Prog, hair progeny; IFE, interfollicular epidermis; JZ, junctional zone; HF, hair follicle; Bulb, hair bulb.

Representative pictures of five mice per genotype. Right: Ki67- (D), γH2AX- (F), and p53- (H) positive cells (% in the indicated compartments) 12 days after plucking.
(I) Left: rhodamine staining of newborn primary keratinocytes undergoing differentiation. Images are representative of five to six mice per genotype. Right: large, differentiated colonies (>3 mm) in differentiating newborn (P1) and adult (P180) mice.
(J) Left: wound healing in *Sox4*^{WT} and *Sox4*^{cKO} mouse skin at D0 and D8. Dashed circles mark the initial wound area. Right: quantification of the remaining wound area (% of initial) at the indicated days. n = 5 mice per genotype unless indicated otherwise. Student's t test was used. Depicted are the average and SEM. Scale bars are included within the micrographs.
See also Figure S4.

Europe PMC Funders Author Manuscripts

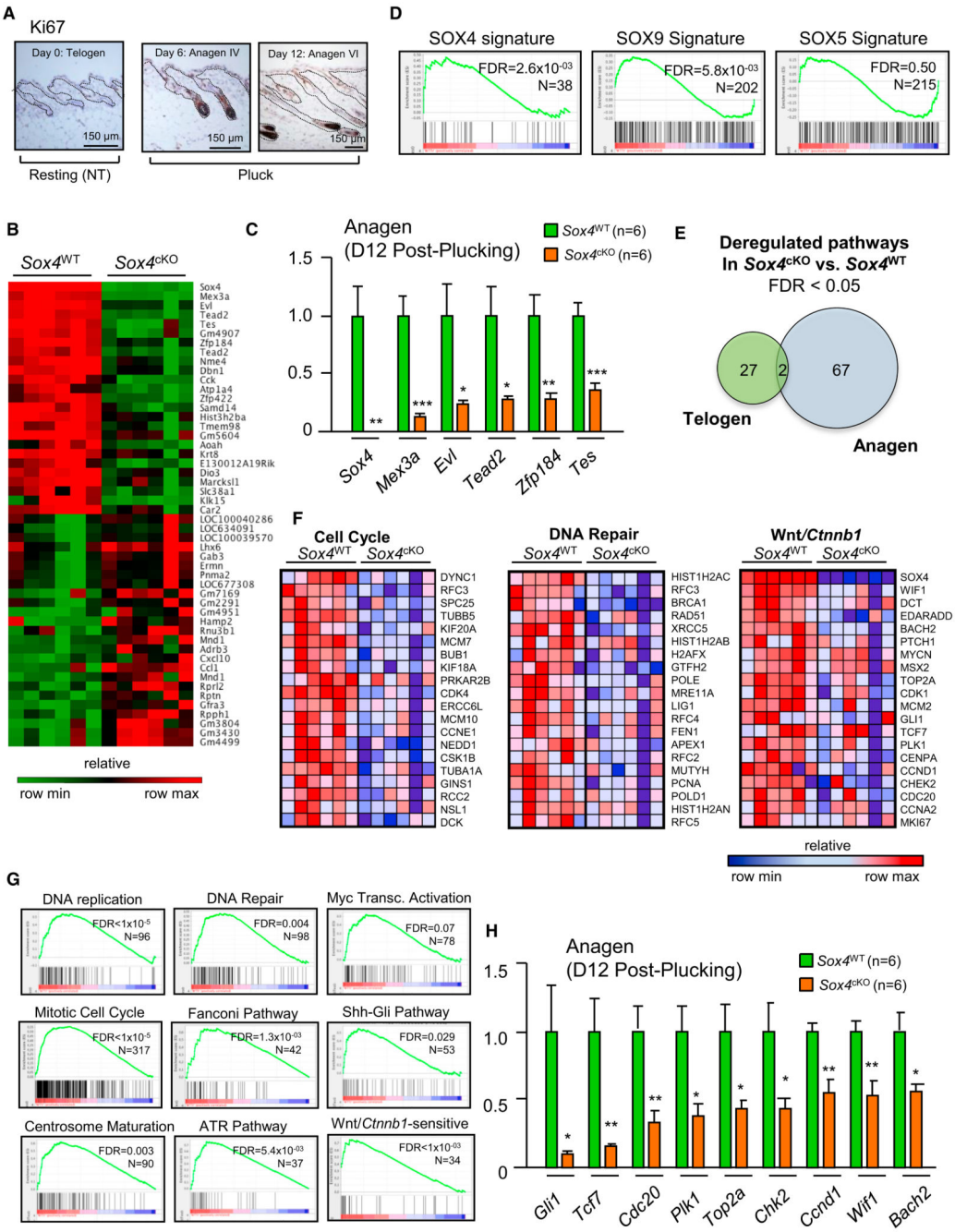

Figure 5. *Sox4* Is Required for the Induction of Proliferative and Differentiation Pathways during Plucking

(A) Ki67 dynamics during plucking, as assessed by IHC.

(B) Heatmap displaying the top 50 DEGs, as estimated by microarray gene profiling, of *Sox4*^{WT} and *Sox4*^{cKO} mice during hair. Gene symbols are shown and relative expression (log_2FC) is scaled in color code (indicated).

(C) qPCR validation of some DEGs found in (B). Depicted is fold over *Sox4*^{WT} for each gene.

Europe PMC Funders Author Manuscripts

(D) Enrichment plots from the Sox4, Sox9, and Sox5 signatures as assessed by GSEA in *Sox4*^{cKO} versus *Sox4*^{WT} mice after plucking.
(E) Venn's diagram comparing differentially downregulated pathways during telogen or anagen in the absence of Sox4.
(F) Heatmaps of the top 20 genes from cell cycle (left), DNA repair (middle), and canonical Wnt/*Ctnnb1* (Lien et al., 2014) (right) pathways, as inferred from GSEA. Relative expression levels are color coded as indicated.
(G) Enrichment plots for the indicated pathways and processes.
(H) qPCR validation of Wnt/*Ctnnb1* genes found downregulated in *Sox4*^{cKO} anagen skin. Depicted is fold over *Sox4*^{WT} for each gene.
The FDR is included for the enrichment plots and number of genes per gene set (n). Student's t test was used for comparison (*$p < 0.05$; **$p < 0.01$; ***$p < 0.001$). Number of mice (n) per genotype is indicated; average and SEM are plotted. See also Figure S5 and Tables S2–S5.

Europe PMC Funders Author Manuscripts

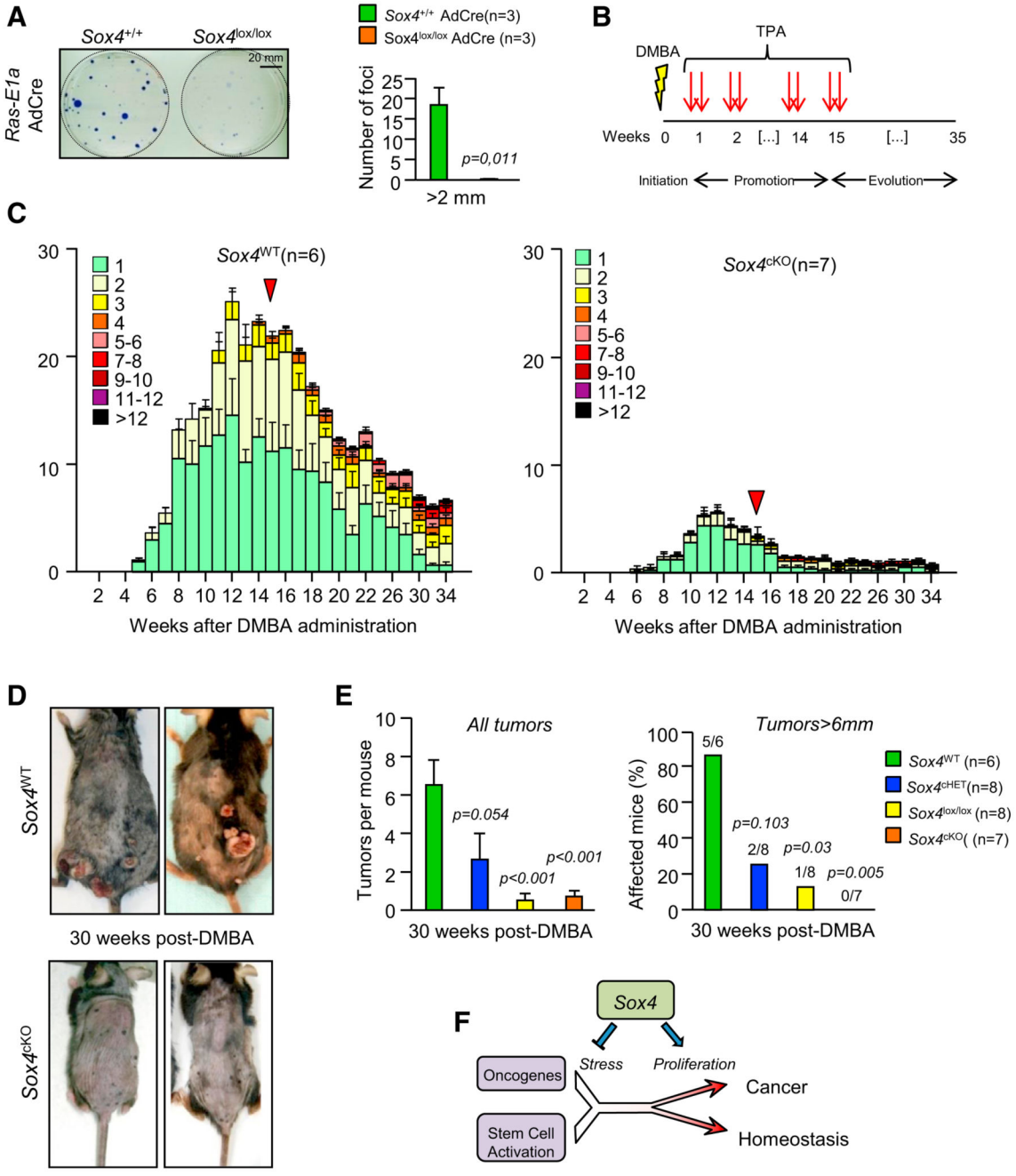

Figure 6.

Sox4 Is Required for Chemically Induced Tumorigenesis

(A) Left: colony-forming assay using transformed *Sox4*$^{+/+}$ and *Sox4*$^{lox/lox}$ MEF transduced with AdCre and Ras-IRES-E1A. Right: number of transformed foci > 2 mm per mouse.

(B) Schematic representation of the TPA/DMBA treatment. Red arrows, twice-weekly administration of TPA.

Europe PMC Funders Author Manuscripts

(C) Average number of tumors, stratified by size (color coded) at the indicated weeks after TPA/DMBA treatment in *Sox4*^{WT} (left) and *Sox4*^{cKO} (right) mice. Red arrowhead, end of the TPA treatment.
(D) *Sox4*^{WT} (top) and *Sox4*^{cKO} mice (bottom) 30 weeks after DMBA treatment.
(E) Average number of tumors (left, Student's t test compared with *Sox4*^{WT}) and percentage of mice bearing tumors > 6 mm (right, Fisher's exact test compared with *Sox4*^{WT}).
(F) Schematic representation of the impact of Sox4 in cancer and aging. n, number of mice per genotype; graphs are mean and SEM. Unless stated otherwise, the statistics used were obtained by Student's t test.
See also Figure S6.

Europe PMC Funders Author Manuscripts